

---

# Generative Imputation and Stochastic Prediction

---

**Mohammad Kachuee, Kimmo Kärkkäinen, Orpaz Goldstein, Sajad Darabi, Majid Sarrafzadeh**

Department of Computer Science

University of California, Los Angeles (UCLA)

{mkachuee, kimmo, orpgol, sajad.darabi}@cs.ucla.edu

## Abstract

In many machine learning applications, we are faced with incomplete datasets. In the literature, missing data imputation techniques have been mostly concerned with filling missing values. However, the existence of missing values is synonymous with uncertainties not only over the distribution of missing values but also over target class assignments that require careful consideration. The objectives of this paper are twofold. First, we proposed a method for generating imputations from the conditional distribution of missing values given observed values. Second, we use the generated samples to estimate the distribution of target assignments given incomplete data. In order to generate imputations, we train a simple and effective generator network to generate imputations that a discriminator network is tasked to distinguish. Following this, a predictor network is trained using imputed samples from the generator network to capture the classification uncertainties and make predictions accordingly. The proposed method is evaluated on CIFAR-10 image dataset as well as two real-world tabular classification datasets, under various missingness rates and structures. Our experimental results show the effectiveness of the proposed method in generating imputations, as well as providing estimates for the class uncertainties in a classification task when faced with missing values.

## 1 Introduction

While a large body of the machine learning literature is built upon the assumption of having access to complete datasets, in many real-world problems only incomplete datasets are available. The existence of missing values can be due to many different causes such as human subjects refusing to answer certain questions or features not being collected frequently due to financial or experimental limitations, sensors failing to record information, and so forth. Data imputation techniques have been suggested as a solution to bridge this gap in the literature via replacing missing values with observed values.

Missing data imputation approaches can be categorized into single and multiple imputation methods. Single imputation methods try to replace each missing value with a plausible value that is the best fit given the value of other correlated features and knowledge extracted from the dataset [1, 2]. While these methods are easy to implement and use in practice, imputed values may induce bias by eliminating less likely but important values. Also, these methods do not suggest a way to measure to what extent the imputed values are representative of the missing values [3].

Multiple imputation (MI) techniques, as suggested by the name, try to use multiple imputed values to impute each missing value. The result would be having a set of imputed datasets that enables measuring how consistent and statistically significant are the results of the experiments [4]. While MI offers interesting statistical insights about the reliability of analysis on incomplete data, the insight is imprecise as it is mainly concerned about the population of data samples rather than individual instances. Specifically, MI methods reason about the statistical properties on a limited number of

imputed datasets (less than 10 in most practical implementations) on the population of samples within the dataset [5, 6].

The existence of missing values is synonymous with having uncertainty over these values that requires careful consideration. Moreover, in many real-world applications we are dealing with supervised problems that demand modeling and prediction based on incomplete data. In this setting, we are not only interested in imputing missing values or measuring how robust our imputations are, but also it is highly desirable to measure the impact of missing values on the prediction outcome for each instance.

In this paper, we propose the idea of Generative Imputation (GI) as a novel approach to impute missing values by sampling from the conditional distributions. Also we suggest a method for measuring how class uncertainties arise from the existence of missing values. The suggested approach is based on neural networks trained using an adversarial objective function. Additionally, a predictor is trained on the generated samples from the imputer network which is able to reflect the impact of uncertainties over missing values. This enables measuring different prediction outcomes and certainties for each specific instance. We evaluate the effectiveness of the proposed method on different incomplete image and tabular datasets under various missingness structures.

## 2 Related Work

One of the simplest traditional methods for handling missing values includes imputing the occurrences of missing values with constant values such as zeros or using mean values. To enhance the accuracy of such imputations, alternatives such as k-nearest neighbors (KNN) [1] and maximum likelihood estimation (MLE) [2] have been suggested to estimate values to be used given an observed context. While these methods are easy to implement and analyze, they often fail to capture the complex feature dependencies as well as structures present in many problems.

Rubin *et al.* [4] suggested a categorization for missingness mechanisms: missing completely at random (MCAR), missing at random (MAR), and missing not at random (MNAR). Under the assumption of MAR, the authors suggested multiple imputation (MI) as a stochastic imputation method. Here, instead of imputing missing values using a single value, it several values are sampled to represent the distribution over the missing value. In this paradigm, MI generates a few imputed complete datasets that are then used independently in statistical modeling [5, 3]. Usually, the final goal of MI is to measure the robustness of the final statistical analysis amongst the imputed datasets. In other words, it measures the quality of imputations and the statistical significance of analysis on the imputed data. It should be noted that the number of imputations used in MI is usually very limited. Also, often strong simplifying assumptions are made in modeling the data distribution (e.g., multi-variate Gaussian or Student's t distribution) which limit the applicability of this method [5, 6].

More recently, autoencoder architectures have been suggested as powerful density estimators capable of capturing complex distributions. Perhaps, denoising autoencoders (DAE) [7] are one of the most intuitive approaches in which a neural network is trained to reconstruct and denoise its input. Following a more probabilistic perspective, variational autoencoders (VAE) [8] try to learn the data generating distribution via a latent representation. Specifically, conditional variational autoencoders (CVAE) [9] can be used to sample missing values conditioned on observed values. For instance, Mattei *et al.* [10] suggested a method based on deep latent variable models and importance sampling that offers a tighter likelihood bound compared to the standard VAE bound. While these methods are powerful generative models applicable to missing data imputation, often samples generated using autoencoders are biased toward the mode of the distribution (e.g., resulting in blurry images, for vision tasks) [11, 12].

Recently, due to the success of generative adversarial networks (GAN), there has been a great attention toward applying these methods for handling missing data. For instance, Yoon *et al.* [13] suggested an imputation method based on adversarial and reconstruction loss terms. Li *et al.* [14] introduced the idea of using separate generator and discriminator networks to learn the missing data structure and data distribution. These methods have been quite successful and are able to present state of the art results. Though it should be noted that often the presence of additional loss terms may bias the generated samples toward the mode of the distribution being modeled. Also, these methods are often very complicated to be applied in practical setups by practitioners. For instance, jointly training multiple generator/discriminator networks, tuning objective functions with multiple hyper-parameters, etc.

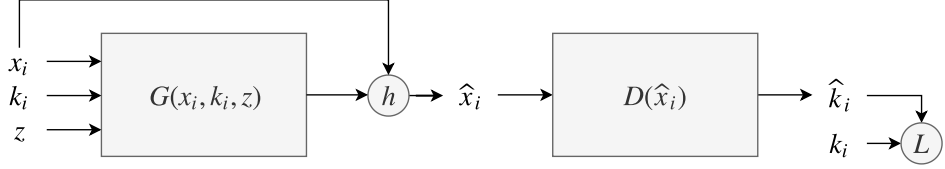


Figure 1: Block diagram of the proposed adversarial imputation method.  $h$  represents the blending function of (1), and  $L$  is the adversarial loss function of (2).

### 3 Proposed Method

#### 3.1 Problem Definition

In this paper, we make the general assumption of having access to an incomplete dataset  $\mathcal{D}$  consisting of a set of feature vector, mask vector, and target class pairs  $(\mathbf{x}_i, \mathbf{k}_i, y_i)$ . For each feature vector,  $\mathbf{x}_i \in \mathbb{R}^d$ , only a subset of the features is available. The mask vector  $\mathbf{k}_i \in \{0, 1\}^d$  is used to indicate available features and missing features by ones and zeros, respectively. Here, to represent features as fixed-width vectors, arbitrary (or NaN) values are used to fill missing values. Also, for convenience, we often use  $\mathbf{x}_i^{obs}$  and  $\mathbf{x}_i^{miss}$  to refer to the set of observed and missing features for the feature vector  $\mathbf{x}_i$ .

In this setting, we define our objective in two steps: (i) Imputing missing values via sampling from the conditional distribution of missing features given observed features i.e.,  $P(\mathbf{x}_i^{miss}|\mathbf{x}_i^{obs})$ . (ii) Estimating the distribution of target classes given the observed features and the distribution of missing features i.e.,  $P(y|\mathbf{x}_i^{obs}, \mathbf{x}_i^{miss})$ . For the first part, we are interested in sampling from the conditional distribution rather than finding the mode of the distribution as the most probable imputation. Similarly, for the second part, we are interested in obtaining a distribution over the possible target assignments and the confidence of each class rather than maximum likelihood class assignments.

#### 3.2 Generative Imputation

In order to generate samples from the distribution of missing features conditioned on the observed features we follow the idea first suggested by Yoon *et al.* [13]. In this paradigm, a generator network is responsible for generating imputations while a discriminator is trying to distinguish imputed features from observed features.

Specifically, the generator function  $G(\mathbf{x}_i, \mathbf{k}_i, \mathbf{z}) \in \mathbb{R}^d$  generates an imputed feature vector, based on observed features, the corresponding mask, and a Gaussian noise vector ( $\mathbf{z}$ ). Note that, in order to achieve the final imputed vector,  $\hat{\mathbf{x}}_i$ , we blend (or, merge) the output of the generator with the input feature to replace generated values with exact value of the observed features:

$$\hat{\mathbf{x}}_{i,j} = \begin{cases} \mathbf{x}_{i,j} & \text{if } \mathbf{k}_{i,j} = 1 \\ G(\mathbf{x}_i, \mathbf{k}_i, \mathbf{z})_j & \text{if } \mathbf{k}_{i,j} = 0 \end{cases}, \quad (1)$$

where  $\mathbf{x}_{i,j}$  refers to  $j$ 'th feature of sample  $i$ . Also, note that by sampling  $\mathbf{z}$  multiple times, we can obtain different imputation samples from the conditional distribution indicated by  $\hat{\mathbf{x}}_i^l$  where  $l$  is the sample number.

A discriminator network,  $D(\hat{\mathbf{x}}_i)$ , is trained to distinguish real and imputed features by generating a predicted softmax mask output,  $\hat{\mathbf{k}}_i$ . Here a binary cross-entropy loss per mask element is used as the adversarial objective function:

$$\max_G \min_D L(G, D) = \mathbb{E}_{\mathbf{k} \sim \mathcal{D}, \hat{\mathbf{k}} \sim D(G(\mathbf{x}, \mathbf{k}, \mathbf{z}))} [\mathbf{k}^T \log(\hat{\mathbf{k}}) + (1 - \mathbf{k})^T \log(1 - \hat{\mathbf{k}})]. \quad (2)$$

The intuition behind this adversarial loss function is that given a generator function which captures the data distribution successfully, the discriminator would not be able to distinguish the parts of the feature vector that were originally missing. While it is quite prevalent in the adversarial learning literature to use additional loss terms such as mean squared error (MSE) to enhance the quality

<b>Algorithm 1:</b> Training the predictor.
<b>Input:</b> $G$ (trained imputer), $\mathcal{D}$ (dataset)
<b>Output:</b> $F_\theta$ (trained predictor)
<b>foreach</b> <i>Training Epoch</i> <b>do</b>
<b>foreach</b> $(\mathbf{x}_i, \mathbf{k}_i, y_i)$ in $\mathcal{D}$ <b>do</b>
$\mathbf{z} \sim N(0, I)$
$\hat{\mathbf{x}}_i \leftarrow \mathbf{k}_i \odot \mathbf{x}_i + (1 - \mathbf{k}_i) \odot G(\mathbf{x}_i, \mathbf{k}_i, \mathbf{z})$
$y_i^{pred} \leftarrow F_\theta(\hat{\mathbf{x}}_i)$
$loss \leftarrow L(y_i, y_i^{pred})$
Backpropagate $loss$
Update $F_\theta$

<b>Algorithm 2:</b> Estimating target distributions.
<b>Input:</b> $F_\theta$ (trained predictor), $(\mathbf{x}, \mathbf{k})$ (test sample), $N$ (ensemble samples)
<b>Output:</b> $\Psi$ (distribution over target classes)
$\Psi \leftarrow zeros \in R^{\#classes}$
<b>foreach</b> Ensemble sample 1 to $N$ <b>do</b>
$\mathbf{z} \sim N(0, I)$
$\hat{\mathbf{x}} \leftarrow \mathbf{k} \odot \mathbf{x} + (1 - \mathbf{k}) \odot G(\mathbf{x}, \mathbf{k}, \mathbf{z})$
$y^{pred} \leftarrow F_\theta(\hat{\mathbf{x}})$
$j \leftarrow argmax(y^{pred})$
$\Psi_j \leftarrow \Psi_j + \frac{1}{N}$

of generated samples, we decided to keep our solution as simple as possible. Additionally, in our experiments, we provide supporting evidence that this simple loss function enables us to sample from the conditional distribution and prevents biased inclinations towards distribution modes.

### 3.3 Stochastic Prediction

In order to realize the second objective of this paper, that is capturing the distribution of target classes given incomplete data, we suggest the idea of stochastic prediction. As indicated in the previous section, the generator can be used to sample from the conditional distribution. Here, a predictor is trained based on the imputed samples to predict class assignments and to calculate the confidence of these assignments. For instance, for a specific test sample at hand, if a certain missing feature is a strong indicator of the target class, we would like to observe the impact of different imputations for that feature on the final hypothesis.

Formally, we are interested in finding the certainty of class assignments given observed and unobserved features:

$$\Psi = P(y|\mathbf{x}_i^{obs}, \mathbf{x}_i^{miss}). \quad (3)$$

Here,  $\Psi$  is a vector where each element is representing a certain class. We use the suggested generative imputation method to sample missing features given observed ones. Rewriting (1) using Hadamard product and as function of the noise vector:

$$\hat{\mathbf{x}}_i = \mathbf{k}_i \odot \mathbf{x}_i + (1 - \mathbf{k}_i) \odot G(\mathbf{x}_i, \mathbf{k}_i, \mathbf{z}) \quad (4)$$

Assuming that a predictor,  $F_\theta$ , is available which predicts class assignments for a complete feature vector,  $\Psi$  can be estimated as:

$$\Psi = \mathbb{E}_{\mathbf{z}}[F_\theta(\hat{\mathbf{x}}_i)] \approx \frac{1}{N} \sum_{l=1}^N F_\theta(\hat{\mathbf{x}}_i^l). \quad (5)$$

Algorithm 1 presents the suggested algorithm for training the predictor. It consists of taking samples from the incomplete dataset, then imputing it with our generator network, and using the imputed sample to update the predictor. Note that, on each epoch and for each sample, the generator generates a new sample from the conditional distribution. Intuitively, it means that the predictor observes and learns to operate under different imputations for a given sample. This is different from approaches such as multiple imputation where several predictors are trained on different imputed versions of a dataset. Algorithm 2 presents the suggested algorithm for making predictions and estimating target distributions given a trained predictor model. Here, a sample is imputed  $N$  times and inference on this set results in an ensemble of predictions over different imputations. The output of this algorithm can be interpreted as a distribution over the confidence of class assignments for a test sample.

### 3.4 Implementation Details

As we conduct experiments on image and tabular datasets, we use different architectures for each. For image datasets, we used a generator and discriminator architectures similar to the ones suggested by Wang *et al.* [15]. However, we improved these architectures using self-attention layers [16]. It should be noted that, while Zhang *et al.* [16] suggests using a single self-attention layer in the middle of

the network, we observed consistent improvements by inserting multiple self-attention layers before each residual block within the network. Furthermore, as input to the generator, we concatenate input image, mask, and a random  $z$  frame along the channels dimension and use it as input. For tabular datasets, we use a simple 4 layer network consisting of fully-connected and batch-norm layers. Also, the input to the generator is the concatenation of a feature vector, mask vector, and a  $z$  vector of size  $\frac{1}{8}$  of the input. For all experiments, we use an ensemble size ( $N$ ) equal to 128.

We used Adam [17] for model optimization. Two time-scale update rule (TTUR) [18] was used to balance training the generator and discriminator networks. We explored best TTUR learning-rate settings from the set of  $\{0.001, 0.0005, 0.0001, 0.00005\}$ . Here, Adam parameters  $\beta_1$  and  $\beta_2$  are set to 0.5 and 0.999, respectively. Also, spectral normalization was used to stabilize both generator and discriminator network in our experiments with image data[19]. For the predictor network, we used the default Adam settings as suggested by Kingma *et al.* [17]. In all training procedures, we decay learning rate by a factor of 5 after reaching a plateau. For all experiments we use a batch size of 64. Based on our experiments, we found that pretraining the discriminator while fixing the generator network for the first 5% of the training epochs helps the stability of training.

Further detail on exact architectures, experiments, software dependencies, etc. as well as ablation studies are provided as supplemental material to this paper.

## 4 Experiments

### 4.1 Datasets

To evaluate the proposed method we use CIFAR-10 [20] as an image classification dataset as well as two tabular datasets: UCI Landsat [21]<sup>1</sup> and Diabetes classification [22] <sup>2</sup>. CIFAR-10 image classification dataset consists of 60,000 32x32 images from 10 different classes. For this task, we use train and test sets as provided by the dataset. As a preprocessing step, we normalize pixel values to the range of  $[0,1]$  and subtract the mean image. The only data augmentation we use for this task is to randomly flip training images for each batch.

UCI Landsat consists of 6435 samples of 36 features from 6 different categories. We follow the same train and test split as provided by the dataset. Diabetes dataset is a real-world health dataset of 92,062 samples and 45 features from different categories such as questionnaire, demographics, medical examination, and lab results. The objective is to classify between three different diabetes conditions i.e., normal, pre-diabetes, and diabetes. As this dataset does not provide explicit train and test sets, we randomly select 80% of samples as a training set and the rest as a test set. To preprocess our tabular datasets, statistical and unity based normalization are used to balance the variance of different features and center them around zero. Also, while different encoding and representation methods are suggested in the literature to handle categorical features [23, 24], in this paper, we take the simple approach of encoding categorical variables using one-hot representation and smoothing them by adding Gaussian noise with zero mean and variance equal to 5% of feature variances. In our experiments, we observed a reasonable performance using the suggested simple smoothing; however, more advanced encoding methods are also applicable in this setup and can be applied to enhance the performances even further.

### 4.2 Missingness Mechanisms

In our experiments, we consider MCAR uniform and MCAR rectangular missingness structures. In MCAR uniform, each feature of each sample is missing based on a Bernoulli distribution with a certain missingness probability (i.e., missing rate) independent of other features. In addition to the case of uniform missingness, for image tasks, we use rectangular missingness/observation structure where rectangular regions of dataset images are missing/observed. In order to control the rate of missingness and decide on the regions that are missing for each case, we use a latent beta distribution that samples rectangular region's width and height such that the average missing rate is maintained. For missing rates less than 50% we make the assumption of having a random rectangular region to be

<sup>1</sup>[https://archive.ics.uci.edu/ml/datasets/Statlog+\(Landsat+Satellite\)](https://archive.ics.uci.edu/ml/datasets/Statlog+(Landsat+Satellite))

<sup>2</sup><https://github.com/mkachuee/Opportunistic>

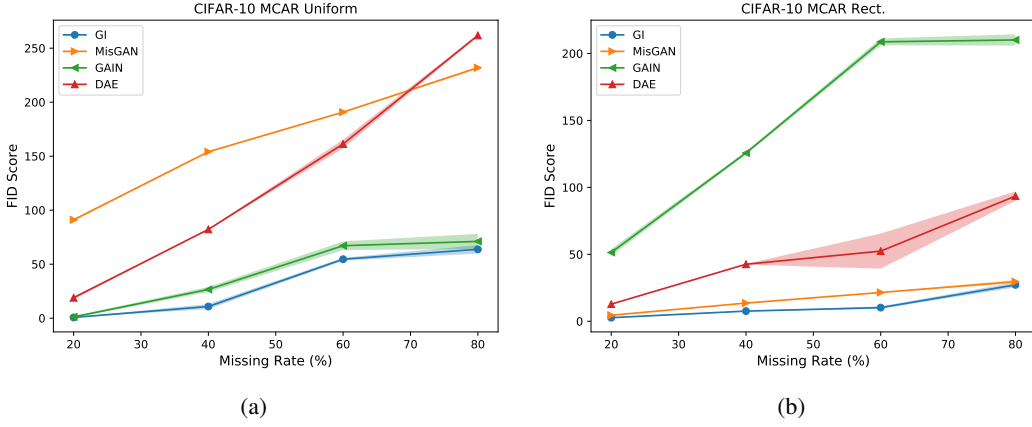


Figure 2: Comparison of FID scores on CIFAR-10 dataset for (a) uniform and (b) rectangular missingness. Lower FID score is better. In many cases, variance values are very small and only observable by magnifying the figures.

missing, whereas for missing rates more than 50% we assume that only a random rectangular region is observed and the rest of the image is missing.

We would like to note that while the suggested solution in this paper is readily compatible with MAR structures, in our experiments, to simplify the presentation of results and to have a fair comparison with other work that do not support the MAR assumption, we limited the scope of our experiments to MCAR. Furthermore, in order to simulate incomplete datasets and to make sure the same features are missing without explicitly storing masks, we use hashed feature vectors to seed random number generators used to sample missing features. More detail is provided as supplemental material.

### 4.3 Evaluation Measures

Fréchet inception distance (FID) [18] score is used to measure the quality of missing data imputation in experiments with images<sup>3</sup>. Also, for each dataset and each missingness scenario we report top-1 classification accuracy based on the majority vote estimated using Algorithm 2. Another measure that we use in this paper is the comparison between the estimated target certainties and average accuracies achieved for each confidence assignment. We run each experiment multiple times (at least 4) and report the mean and standard deviation of results for each case.

We compare our results with MisGAN [14] and GAIN [13] as the state of the art imputation algorithms based on GANs as well as basic denoising autoencoder (DAE) [7] as baselines. For experiments using MisGAN, we used the same architectures and hyper-parameters as suggested by the MisGAN authors<sup>4</sup>. The only modification was to adapt the last generator layer to generate images with resolutions as we use. Regarding GAIN, we used the same network architecture as our implementation of GI and hyper-parameters as used by the GAIN authors<sup>5</sup>. In the DAE implementation, due to the incomplete data assumption, only observed features appear in the loss function, ignoring reconstruction terms corresponding to missing features.

### 4.4 Results

Figure 2 presents the comparison of FID scores on the CIFAR-10 dataset at different missing rates for uniform and rectangular missingness. As it can be inferred from these plots, GI outperforms other alternatives in all cases. Also, it can be seen that GAIN is able to provide more reasonable results for uniform missing data structure compared to MisGAN which is mainly effective in rectangular missing data structure. One possible explanation for this behavior might be the fact that GAIN has MSE loss terms that would act as a denoising loss smoothing noisy missing pixels. On the other hand, MisGAN tries to explicitly model missingness structure and is more successful in capturing a

<sup>3</sup><https://github.com/mseitzer/pytorch-fid> is adapted to measure the FID scores.

<sup>4</sup><https://github.com/steveli/misgan>

<sup>5</sup><https://github.com/jsyoon0823/GAIN>

Table 1: Top-1 CIFAR-10 classification accuracy for different missing rates and structures.

Method	Accuracy at Missing Rate (%)							
	MCAR Uniform				MCAR Rect.			
	20%	40%	60%	80%	20%	40%	60%	80%
GI	<b>89.5</b> ( $\pm 0.45$ )	<b>87.1</b> ( $\pm 0.54$ )	80.3 ( $\pm 0.26$ )	76.0 ( $\pm 1.05$ )	<b>84.0</b> ( $\pm 0.03$ )	<b>76.9</b> ( $\pm 0.03$ )	<b>66.1</b> ( $\pm 0.16$ )	<b>46.0</b> ( $\pm 0.76$ )
MisGAN	87.6 ( $\pm 0.04$ )	85.2 ( $\pm 0.38$ )	81.1 ( $\pm 0.41$ )	72.7 ( $\pm 0.03$ )	83.5 ( $\pm 0.40$ )	76.5 ( $\pm 0.48$ )	65.3 ( $\pm 0.32$ )	43.5 ( $\pm 0.01$ )
GAIN	89.4 ( $\pm 0.41$ )	86.0 ( $\pm 0.06$ )	<b>81.9</b> ( $\pm 0.48$ )	<b>78.5</b> ( $\pm 0.15$ )	82.2 ( $\pm 0.07$ )	75.3 ( $\pm 0.67$ )	59.2 ( $\pm 1.03$ )	38.1 ( $\pm 1.59$ )
DAE	88.0 ( $\pm 0.22$ )	84.0 ( $\pm 0.50$ )	79.8 ( $\pm 0.71$ )	71.9 ( $\pm 0.28$ )	83.3 ( $\pm 0.64$ )	75.5 ( $\pm 0.44$ )	63.8 ( $\pm 0.24$ )	42.7 ( $\pm 1.07$ )

Table 2: Comparison of classification accuracies for Landsat and Diabetes datasets at different missing rates.

Dataset	Method	Accuracy at Missing Rate (%)				
		10%	20%	30%	40%	50%
Landsat [21]	GI	<b>89.3</b> ( $\pm 0.35$ )	<b>88.7</b> ( $\pm 0.24$ )	<b>87.7</b> ( $\pm 0.26$ )	<b>86.5</b> ( $\pm 0.21$ )	82.9 ( $\pm 0.36$ )
	MisGAN [14]	88.3 ( $\pm 1.03$ )	86.9 ( $\pm 1.16$ )	87.1 ( $\pm 0.94$ )	84.6 ( $\pm 1.96$ )	82.2 ( $\pm 1.07$ )
	GAIN [13]	89.1 ( $\pm 0.40$ )	88.4 ( $\pm 0.30$ )	86.9 ( $\pm 0.20$ )	86.3 ( $\pm 0.41$ )	<b>84.4</b> ( $\pm 0.80$ )
	DAE [7]	88.4 ( $\pm 0.47$ )	86.9 ( $\pm 0.70$ )	85.5 ( $\pm 0.39$ )	84.5 ( $\pm 0.21$ )	82.9 ( $\pm 0.70$ )
Diabetes [22]	GI	89.0 ( $\pm 0.25$ )	87.9 ( $\pm 0.36$ )	<b>87.1</b> ( $\pm 0.53$ )	<b>86.0</b> ( $\pm 0.60$ )	<b>84.9</b> ( $\pm 0.42$ )
	MisGAN [14]	<b>89.1</b> ( $\pm 0.25$ )	<b>88.3</b> ( $\pm 0.24$ )	<b>87.1</b> ( $\pm 0.46$ )	85.3 ( $\pm 0.33$ )	83.7 ( $\pm 2.47$ )
	GAIN [13]	88.9 ( $\pm 0.15$ )	87.8 ( $\pm 0.26$ )	86.5 ( $\pm 0.24$ )	84.6 ( $\pm 1.36$ )	82.8 ( $\pm 1.13$ )
	DAE [7]	88.7 ( $\pm 0.11$ )	87.6 ( $\pm 0.29$ )	86.5 ( $\pm 0.13$ )	85.5 ( $\pm 0.09$ )	83.9 ( $\pm 0.31$ )

more structured missingness such as the case of rectangular structure. Table 1 provides a comparison between the top-1 classification accuracy achieved using each method at different missing rates and structures. From this table, GI outperforms other work by achieving best results in 6 out of 8 cases.

Table 2 presents a comparison of classification accuracies for Landsat and Diabetes datasets at different missing rates. In the Landsat benchmark, GI outperforms other work in 4 out of 5 cases. However, in the diabetes classification task, GI appears to be more effective imputing missing rates more than 30% while MisGAN provides better or similar results at lower missing rates.

Figure 3 shows a comparison of accuracy versus certainty plots for GI, MisGAN, and GAIN on Landsat dataset at the missing rate of 40%. To generate these figures we trained each imputation method and then used Algorithm 1 to train predictors on imputed samples. Finally, Algorithm 2 used to measure the average accuracy at different prediction confidence levels based on a sample of 128 imputations for each test example. As it can be seen from the plots, GI provides results closest to the ideal case of having average confidence values equal to average accuracies.

#### 4.5 Visualization using Synthesized Data

In order to provide further insight into the operation of GI and how imputations can potentially influence the outcomes of predictions, we conduct experiments on a synthesized dataset. The original underlying data distribution is generated by sampling 5000 samples from 4 Gaussians of standard deviation 0.1 centered on the vertices of a unit square. We assign two different classes to each cluster such that diagonal vertices are of the same class (see Figure 4a, classes are represented with colors). From this underlying distribution we make an incomplete dataset with 50% of values missing.

The incomplete synthesized dataset is used to train GI and other imputation methods. We take a random test sample in which the second feature has a value of about 0.1 and the other feature is missing. Ideally, in the imputation phase, we would like to sample from the condition distribution i.e.  $P(x_1|x_2 = 0.1)$  (see Figure 4b). In this case, in the prediction phase, an ideal method would decide on not making a confident classification and report the uncertainty. Note that solely observing the value of 0.1 for the second feature does not provide any useful evidence for the prediction. Figure 4c-f provide samples and classification results for GI, MisGAN, GAIN, and DAE. As it can be inferred from these figures, GI generates reasonable samples from the conditional distribution and also reflects

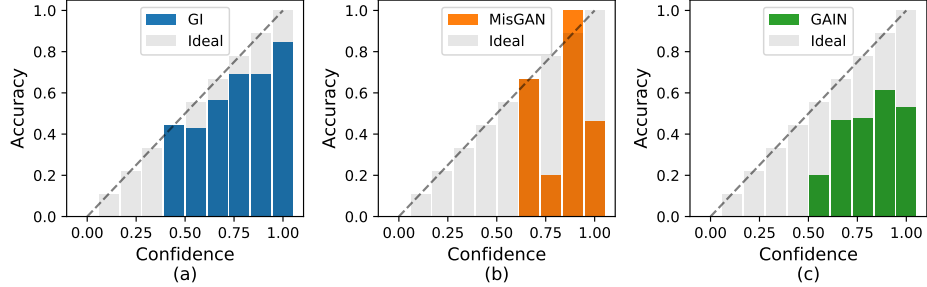


Figure 3: Accuracy versus certainty plots for (a) GI, (b) MisGAN, and (c) GAIN on Landsat dataset at the missing rate of 40%.

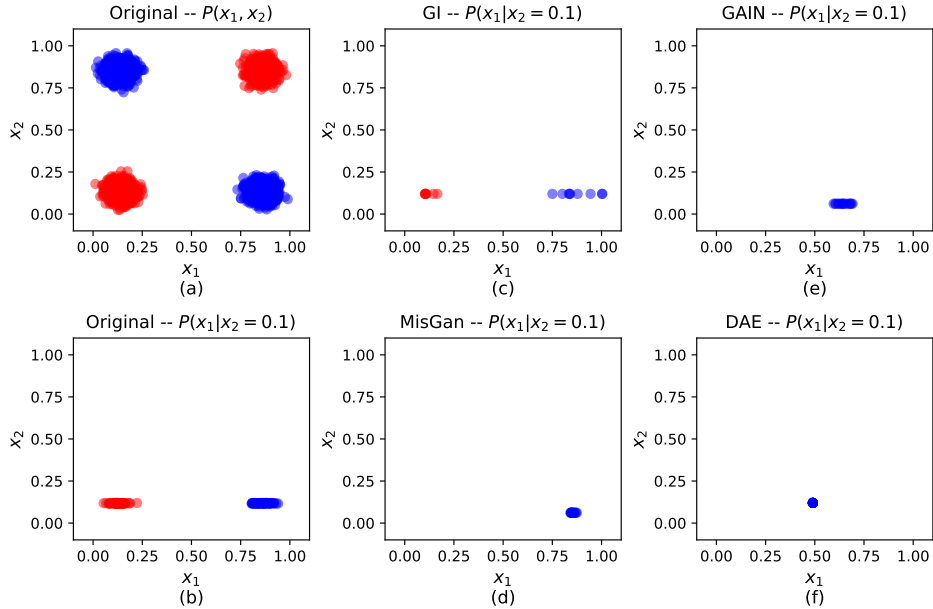


Figure 4: Evaluation using synthesized data: (a) samples from the underlying distribution, (b) samples from the conditional underlying distribution, (c-f) samples from the conditional distribution generate by GI, MisGAN, GAIN, and DAE.

this uncertainty over the prediction. On the other hand MisGAN, probably due to its complexity of using 3 different generators and discriminator pairs, is suffering from mode collapse and is unable to generate samples from the other class, resulting in over-confident assignments. GAIN, perhaps due to the MSE loss terms, is inclined towards the mean of the conditional distribution at the origin. DAE, as expected, due to its MSE loss term, only captures the expected value of the distribution mean hence reducing the MSE error and generates over-smoothed imputations.

## 5 Conclusion

In this paper we proposed a novel method to generate imputations and measure uncertainties over target class assignments based on incomplete feature vectors. We evaluated the effectiveness of the suggested approach on image and tabular data via using different measures such as FID distance, classification accuracy, and confidence versus accuracy plots. According to the experiments, the proposed method not only is able to generate accurate imputations outperforming state of the art imputation techniques, but also to model prediction uncertainties arising from missing values. The proposed method is applicable to many real-world applications where only an incomplete dataset is available, and modeling classification uncertainties is a necessity.

## References

- [1] Trevor Hastie, Robert Tibshirani, Gavin Sherlock, Michael Eisen, Patrick Brown, and David Botstein. Imputing missing data for gene expression arrays, 1999.
- [2] Theodore W Anderson. Maximum likelihood estimates for a multivariate normal distribution when some observations are missing. *Journal of the american Statistical Association*, 52(278):200–203, 1957.
- [3] Roderick JA Little and Donald B Rubin. *Statistical analysis with missing data*, volume 793. Wiley, 2019.
- [4] Donald B Rubin. Inference and missing data. *Biometrika*, 63(3):581–592, 1976.
- [5] Joseph L Schafer and John W Graham. Missing data: our view of the state of the art. *Psychological methods*, 7(2):147, 2002.
- [6] Jared S Murray et al. Multiple imputation: a review of practical and theoretical findings. *Statistical Science*, 33(2):142–159, 2018.
- [7] Pascal Vincent, Hugo Larochelle, Yoshua Bengio, and Pierre-Antoine Manzagol. Extracting and composing robust features with denoising autoencoders. In *Proceedings of the 25th international conference on Machine learning*, pages 1096–1103. ACM, 2008.
- [8] Diederik P Kingma and Max Welling. Auto-encoding variational bayes. *arXiv preprint arXiv:1312.6114*, 2013.
- [9] Kihyuk Sohn, Honglak Lee, and Xinchen Yan. Learning structured output representation using deep conditional generative models. In *Advances in neural information processing systems*, pages 3483–3491, 2015.
- [10] Pierre-Alexandre Mattei and Jes Frellsen. missiwa: Deep generative modelling and imputation of incomplete data. *arXiv preprint arXiv:1812.02633*, 2018.
- [11] Ian Goodfellow, Jean Pouget-Abadie, Mehdi Mirza, Bing Xu, David Warde-Farley, Sherjil Ozair, Aaron Courville, and Yoshua Bengio. Generative adversarial nets. In *Advances in neural information processing systems*, pages 2672–2680, 2014.
- [12] Vincent Dumoulin, Ishmael Belghazi, Ben Poole, Olivier Mastropietro, Alex Lamb, Martin Arjovsky, and Aaron Courville. Adversarially learned inference. *arXiv preprint arXiv:1606.00704*, 2016.
- [13] Jinsung Yoon, James Jordon, and Mihaela Van Der Schaar. Gain: Missing data imputation using generative adversarial nets. *arXiv preprint arXiv:1806.02920*, 2018.
- [14] Steven Cheng-Xian Li, Bo Jiang, and Benjamin Marlin. Learning from incomplete data with generative adversarial networks. In *International Conference on Learning Representations*, 2019.
- [15] Ting-Chun Wang, Ming-Yu Liu, Jun-Yan Zhu, Andrew Tao, Jan Kautz, and Bryan Catanzaro. High-resolution image synthesis and semantic manipulation with conditional gans. In *Proceedings of the IEEE Conference on Computer Vision and Pattern Recognition*, pages 8798–8807, 2018.
- [16] Han Zhang, Ian Goodfellow, Dimitris Metaxas, and Augustus Odena. Self-attention generative adversarial networks. *arXiv preprint arXiv:1805.08318*, 2018.
- [17] Diederik P Kingma and Jimmy Ba. Adam: A method for stochastic optimization. *arXiv preprint arXiv:1412.6980*, 2014.
- [18] Martin Heusel, Hubert Ramsauer, Thomas Unterthiner, Bernhard Nessler, and Sepp Hochreiter. Gans trained by a two time-scale update rule converge to a local nash equilibrium. In *Advances in Neural Information Processing Systems*, pages 6626–6637, 2017.

- [19] Takeru Miyato, Toshiki Kataoka, Masanori Koyama, and Yuichi Yoshida. Spectral normalization for generative adversarial networks. *arXiv preprint arXiv:1802.05957*, 2018.
- [20] Alex Krizhevsky and Geoffrey Hinton. Learning multiple layers of features from tiny images. Technical report, Citeseer, 2009.
- [21] Dheeru Dua and Casey Graff. UCI machine learning repository, 2017.
- [22] Mohammad Kachuee, Kimmo Karkkainen, Orpaz Goldstein, Davina Zamanzadeh, and Majid Sarrafzadeh. Nutrition and health data for cost-sensitive learning. *arXiv preprint arXiv:1902.07102*, 2019.
- [23] Eric Jang, Shixiang Gu, and Ben Poole. Categorical reparameterization with gumbel-softmax. *arXiv preprint arXiv:1611.01144*, 2016.
- [24] Alfredo Nazabal, Pablo M Olmos, Zoubin Ghahramani, and Isabel Valera. Handling incomplete heterogeneous data using vaes. *arXiv preprint arXiv:1807.03653*, 2018.

---

# Supplemental Material for: Generative Imputation and Stochastic Prediction

---

**Mohammad Kachuee, Kimmo Kärkkäinen, Orpaz Goldstein, Sajad Darabi, Majid Sarrafzadeh**

Department of Computer Science

University of California, Los Angeles (UCLA)

{mkachuee,kimmo,orpgol,sajad.darabi}@cs.ucla.edu

## Appendices

### Contents

<b>Appendices</b>	<b>1</b>
<b>A Implementation and Experiments</b>	<b>2</b>
<b>B Network Architectures</b>	<b>2</b>
<b>C Missing Data Mechanisms</b>	<b>3</b>
<b>D Ablation Study</b>	<b>5</b>

## A Implementation and Experiments

Table 1 presents the list of dependencies and versions used in the provided implementation. To produce results related to this paper, we used a workstation with 4 NVIDIA GeForce RTX-2080Ti GPUs, a 12 core Intel Core i9-7920X processor, and 128 GB memory. Each single experiment took between about 4 hours to 48 hours, based on the task and method begin tested.

Table 1: Software dependencies.

Dependency	Version
python	3.7.1
pytorch	1.0.0
cuda100	1.0
ipython	7.2.0
jupyter	1.0.0
numpy	1.15.4
pandas	0.24.1
scikit-learn	0.20.1
scipy	1.1.0
torchvision	0.2.1
tqdm	4.28.1
matplotlib	3.0.1

## B Network Architectures

Table 2 shows the exact architectures used in this paper. To show each layer or block we used the following notation.  $CxSyPz-t$  represents a 2-d convolution layer of kernel size  $x$ , stride  $y$ , padding  $z$ , and number of output channels  $t$  followed by ReLU activation.  $Attn$  represents a self-attention layer similar to Zhang *et al.*<sup>1</sup>.  $R-x$  represents a residual block consisting of two 2-d convolutions with kernel size 3 (padding size 1), batch normalization, and ReLU activation.  $CTxSyPz-t$  is the convolution transpose corresponding to  $CxSyPz-t$ .  $FC-x$  is representing a linear fully-connected layer of  $x$  output neurons with biases. We use spectral normalization as suggested by Miyato *et al.*<sup>2</sup> for all convolutional layers in both generator and discriminator networks.

Table 2: Network architectures used in our experiments.

Dataset	Generator/Discriminator Architecture	Predictor Architecture
<b>CIFAR-10</b>	$C7S1P3-64, C3S2P1-128, Attn, R-128,$	ResNet-18 <sup>3,4</sup>
	$Attn, R-128, Attn, R-128, Attn,$	
	$R-128, CT3S2P1-128, CT7S1P3-3, Tanh/Sigmoid$	
<b>Landsat</b>	$FC-36, Sigmoid, BN, FC-36, Sigmoid, BN,$ $FC-36, Sigmoid, BN, FC-36, Tanh/Sigmoid$	$FC-18, ReLU, BN, FC-18,$ $ReLU, BN, FC-6, Softmax$
<b>Diabetes</b>	$FC-45, ReLU, BN, FC-45, ReLU, BN,$ $FC-45, ReLU, BN, FC-45, Tanh/Sigmoid$	$FC-22, ReLU, BN, FC-22,$ $ReLU, BN, FC-3, Softmax$

<sup>1</sup>Zhang, Han, et al. "Self-attention generative adversarial networks." arXiv preprint arXiv:1805.08318 (2018).

<sup>2</sup>Miyato, Takeru, et al. "Spectral normalization for generative adversarial networks." arXiv preprint arXiv:1802.05957 (2018).

<sup>3</sup>He, Kaiming, et al. "Deep residual learning for image recognition." Proceedings of the IEEE conference on computer vision and pattern recognition. 2016.

<sup>4</sup><https://github.com/kuangliu/pytorch-cifar>

## C Missing Data Mechanisms

In this paper, we conduct experiments on two mechanisms for missing values: MCAR uniform and MCAR rectangular. As in our experiments and comparisons we consider the case where only an incomplete dataset is available for training. It is crucial to guarantee that each method has only access to a unique incomplete version of each sample. However, it is relatively expensive to load and store feature masks for each sample in the dataset. Instead, we generate missing values during the data load for each batch. A hashing mechanism is used to ensure that the exact same parts are missing for each sample throughout the training. Note that we set system, python, and external library hash seeds to fixed values to ensure the consistency between different runs.

Algorithm 1 presents the procedure used for generating missing values with uniform structure. This algorithm is sampling independent Bernoulli distributions with probabilities equal to the missing rate. Algorithm 2 shows the outline for the rectangular missing structure used in image experiments. It consists of selecting a random point as the center of the rectangle and then deciding on parameters to be used for the beta distribution based on the missing rate. Finally, width and height of the rectangular region are sampled from the latent beta distribution. In other words, we generate rectangular regions centered at random locations within the image which have width and height values determined by samples from a latent beta distribution. Here, distribution parameters,  $\alpha$  and  $\beta$ , are used to control the average missing rate. The final outcome would be rectangular regions of different shape at different locations within the frame with expected portion of missing area equal to the missing rate.

In order to decide on the beta distribution parameters i.e.  $\alpha$  and  $\beta$  we use numerical simulations. Specifically, we fix one of the parameters to 1 and change the other parameter in the range of [1,10], while measuring the average missing rate caused by each case. Figure 1 shows the missing rates caused by different beta distribution parameters. In this figure, the first half (missing rates less than about 0.18) corresponds to setting  $\beta$  to 1 and changing  $\alpha$  values; and the other half fixing  $\alpha$  to 1 and changing  $\beta$  values. To generate missing rates more than 50% we invert our masks and limit the observation to the rectangular region while the rest of the image is missing. Note that missing rates indicate the ratio of feature that are missing on average case. As we are using a latent model for sampling width and height for the rectangles, the actual missing ratios for each specific sample differs between samples. See Table 3 for visual examples of different missing rates and missing structures.

---

### Algorithm 1: MCAR uniform generation.

---

**Input:**  $x$  (complete feature),  $r$  (missing rate)  
**Output:**  $x_m$  (incomplete feature)  
 $seed_x \leftarrow \text{hash}(x)$   
 $\mathbf{k} \leftarrow 1 - \text{Bernoulli}(seed_x, \text{shape}(x), \text{prob} = r)$   
 $x_m \leftarrow \mathbf{k} \odot x + (1 - \mathbf{k}) \odot \text{NaN}$

---



---

### Algorithm 2: MCAR rect. generation.

---

**Input:**  $x$  (complete feature),  $r$  (missing rate)  
**Output:**  $x_m$  (incomplete feature)  
 $seed_x \leftarrow \text{hash}(x)$   
 $n_x, n_y \leftarrow \text{shape}(x)$   
 $(p_x, p_y) \sim (\text{uniform}(0, n_x), \text{uniform}(0, n_y))$   
 $\alpha, \beta \leftarrow \text{beta\_params}(r) // \text{beta\_params gives } \alpha, \beta \text{ for each}$   
 $\text{missing rate based on numerical simulations}$   
 $(w, h) \sim (\text{Beta}(\alpha, \beta) \times n_x, \text{Beta}(\alpha, \beta) \times n_y)$   
 $\mathbf{k} \leftarrow \text{rect\_mask}(p_x, p_y, w, h)$   
 $x_m \leftarrow \mathbf{k} \odot x + (1 - \mathbf{k}) \odot \text{NaN}$

---

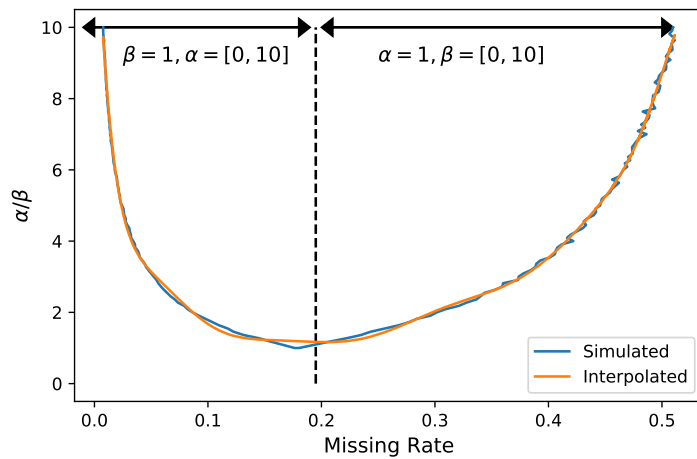


Figure 1: Simulation results for measuring average missing rate given different beta distribution parameters.

Table 3: Examples of uniform and rectangular missing structures at different missing rates.

	Original	20 %	40 %	60 %	80 %
Uniform					
Rect.					

## D Ablation Study

Figure 2 presents a comparison between using (GI W/ Atten.) and not using (GI W/O Atten.) self-attention layers before each residual block in the proposed architecture. We report FID scores on CIFAR-10 with rectangular missingness. As it can be inferred from this comparison, using self-attention achieves a consistent improvement over the baseline. We also examined the case of uniform missingness; however, we did not observe any significant improvement for this case. One possible explanation could be the fact that imputing missing data with a uniform structure can be done by processing local regions and does not require attending to different distant regions across the image.

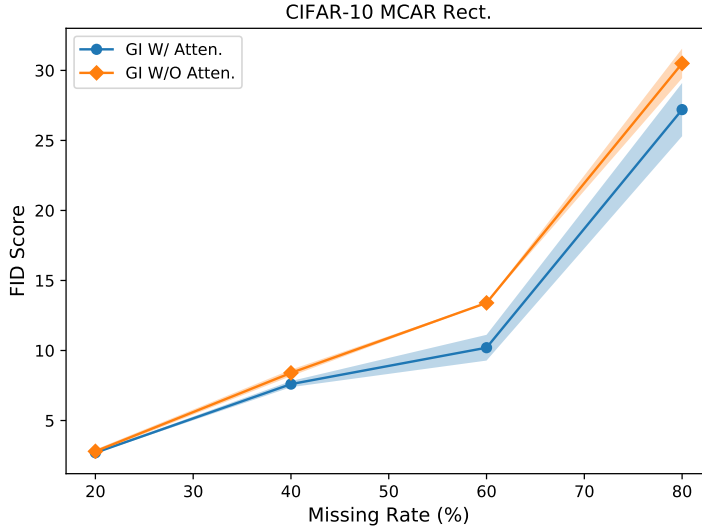


Figure 2: Comparison of FID scores achieved with (GI W/ Atten.) and without (GI W/O Atten.) self-attention layers on CIFAR-10 dataset and rectangular missingness. Lower FID score is better.

Figure 3 shows a comparison of classification accuracies for the Landsat dataset achieved using different ensemble sizes ( $N$ ). As it can be seen from this figure, higher values of  $N$  result in improved accuracies specially for higher missing rates. Also, it can be observed that for  $N$  values more than 64 the difference is negligible.

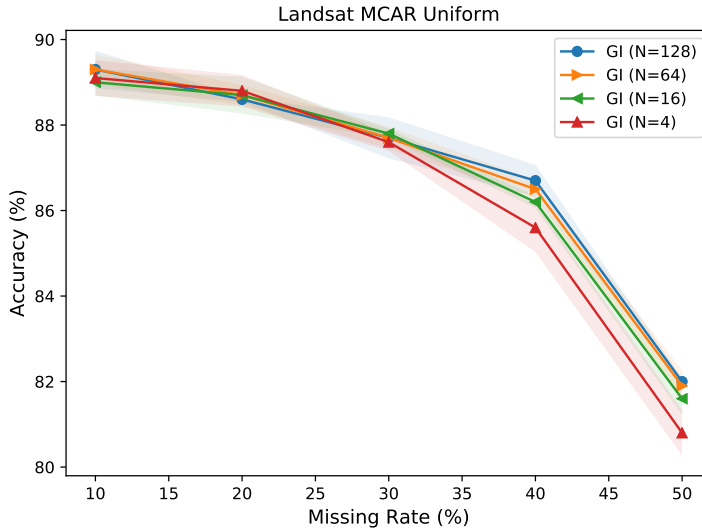


Figure 3: Comparison of classification accuracies achieved with different ensemble size ( $N$ ).